Local Order and Metal−Metal Bonding in Li_2MoO_3, $Li_4Mo_3O_8$, $LiMoO_2$, and H_2MoO_3, Determined from EXAFS Studies

S. J. Hibble* and I. D. Fawcett

Department of Chemistry, University of Reading, Whiteknights, P.O. Box 224, Reading RG6 2AD, England

Received August 3, 1994[⊗]

Molybdenum K-edge EXAFS studies have allowed us to determine the local order in the layered materials Li_2MoO_3, $Li_4Mo_3O_8$, $LiMoO_2$, and H_2MoO_3. The presence of Mo_3 metal−metal-bonded triangles in Li_2MoO_3, with d(Mo−Mo) = 2.580(1) Å (×2), is unequivocally demonstrated for the first time. This information cannot be obtained from diffraction experiments because the system is intrinsically disordered. Triangular clusters are also found in the related Mo^{IV}-containing lithium molybdate $Li_4Mo_3O_8$ and in H_2MoO_3, prepared from Li_2MoO_3 by ion exchange (d(Mo−Mo) = 2.560(1) Å (×2) and 2.506(1) Å (×2), respectively). The metal−metal bonding in the Mo^{III}-containing oxide $LiMoO_2$ is shown to be more complex than diffraction studies had indicated. In $LiMoO_2$, Mo−Mo-bonded chains are formed, and we present a possible model containing disordered chains, with d(Mo−Mo) = 2.561(2) Å (×2) and 2.709(2) Å (×2), found in the MoO_2 sheets.

Introduction

Metal−metal-bonded clusters are the subject of wide interest in the chemistry of molecules and extended solids. Trinuclear M_3 clusters, by definition the smallest clusters, were first found in metal oxide chemistry with the synthesis of $Zn_2Mo_3O_8$ by McCarroll, Katz, and Ward in 1957.[1] The Mo_3O_{13} cluster (Figure 1) is now known in a wide range of compounds.[2−4] In addition to the simple Mo_3 cluster, many higher nuclearity clusters are now known in mixed-metal oxides containing molybdenum. These include Mo_4, Mo_6, Mo_8, and Mo_{10} clusters,[5−7] both isolated and condensed to form larger units such as infinite chains. Examples of infinite-chain compounds include $NaMo_2O_4$ and $Li_{0.74}MoO_2$.[8,9]

The lithium−molybdenum−oxygen phase diagram includes compounds of Mo^{IV}, Li_2MoO_3 and $Li_4Mo_3O_8$,[10−12] which might be expected to contain Mo_3 triangles, and Mo^{III}, $LiMoO_2$,[9] which might be expected to contain more complex units. The structures of Li_2MoO_3 and $LiMoO_2$ have been determined by powder neutron diffraction.[13,9] Both compounds contain cubic close-packed layers of oxygen with lithium and molybdenum in octahedral sites (Figure 2). In $LiMoO_2$, lithium and molybdenum are ordered to give hexagonal sheets of Li^I and Mo^{III} in alternate layers. The published crystal structure contains infinite hexagonal sheets, with each Mo having six near neighbors at 2.866 Å. A notable features of the structure refinement is the very high isotropic temperature factor for molybdenum, which suggests that some static disorder unaccounted for in the structural model may be present. Indeed, the authors' own extended Hückel calculations predict that the Mo layers should distort.

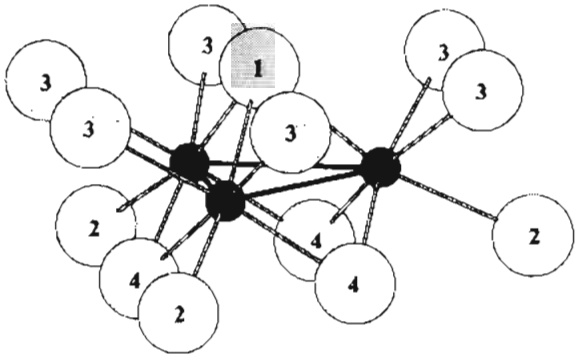

Figure 1. The Mo_3O_{13} unit in $Zn_2Mo_3O_8$ (solid circles, Mo; open circles, O) showing the numbering scheme used in the text.

Li_2MoO_3 has a slightly more complicated structure, containing mixed Mo^{IV}/Li^I layers in addition to Li layers. The formula $Li[Mo_{2/3}Li_{1/3}]O_2$ shows the relationship between the materials. In this case, James and Goodenough suggest the material contains disordered Mo_3 clusters, but although their evidence from photoelectron spectroscopy would support this hypothesis, their structural model does not include such units. Two compounds closely related to Li_2MoO_3 are H_2MoO_3, prepared by proton exchange,[14] and another lithium molybdate, $Li_4Mo_3O_8$,[12] prepared in the reinvestigation of the $Li_2O−MoO_2$ phase diagram. Both compounds contain Mo^{IV}, and powder

[⊗] Abstract published in *Advance ACS Abstracts*, January 1, 1995.

(1) McCarroll, W. H.; Katz, L.; Ward, R. *J. Am. Chem. Soc.* **1957**, *79*, 5410.
(2) McCarroll, W. H. *Inorg. Chem.* **1977**, *16*, 3351.
(3) Betteridge, P. W.; Cheetham, A. K.; Howard, J. A. K.; Jakubicki, G.; McCarroll, W. H. *Inorg. Chem.* **1984**, *23*, 737.
(4) Torardi, C. C.; McCarley, R. E. *Inorg. Chem.* **1985**, *24*, 476.
(5) McCarley, R. E.; Lii, K.-H.; Edwards, P. A.; Brough, L. F. *J. Solid State Chem.* **1985**, *57*, 17.
(6) Gougeon, P.; McCarley, R. E. *Acta Crystallogr., Sect. C: Cryst. Struct. Commun.* **1991**, *21*, 241.
(7) Hibble, S. J.; Cheetham, A. K.; Bogle, A. R. L.; Wakerley, H. R.; Cox, D. E. *J. Am. Chem. Soc.* **1988**, *110*, 3295.
(8) Torardi, C. C.; McCarley, R. E. *J. Am. Chem. Soc.* **1979**, *101*, 3963.
(9) Aleandri, L. E.; McCarley, R. E. *Inorg. Chem.* **1988**, *27*, 1041.
(10) Gleitzer, C. *Bull. Soc. Chim. Fr.* **1966**, *6*, 1913.
(11) Reau, J. M.; Fouassier, C.; Gleitzer, C. *Bull. Soc. Chim. Fr.* **1967**, *11*, 4294.
(12) McGrellis, S. A. Ph.D. Thesis, University of Reading, Reading, U.K., 1994.
(13) James, A. C. W. P.; Goodenough, J. B. *J. Solid State Chem.* **1988**, *76*, 87.
(14) Gopalakrishnan, J.; Bhat, V. *Mater. Res. Bull.* **1987**, *22*, 769.

0020-1669/95/1334-0500$09.00/0

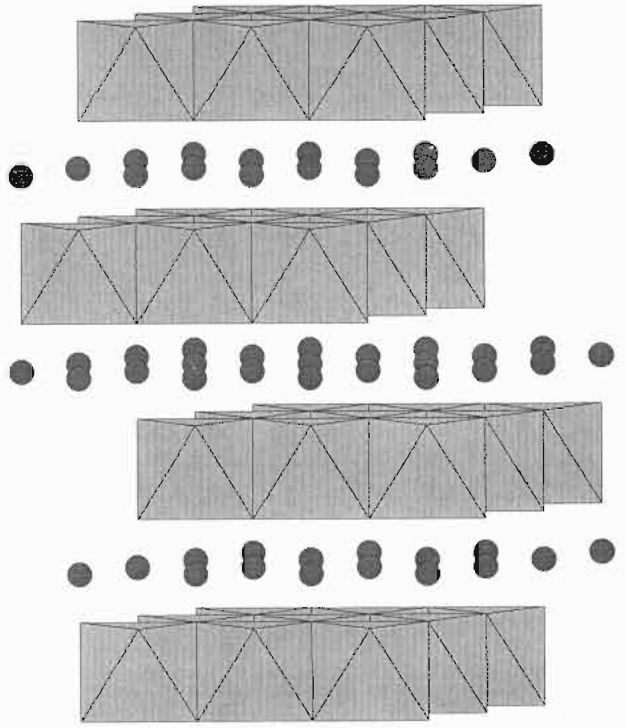

Figure 2. Layer structure of $LiMoO_2$ and Li_2MoO_3. Shaded octahedra show the MO_2 layer (in $LiMoO_2$ (M = Mo) and in Li_2MoO_3 (M = $Mo_{2/3}Li_{1/3}$)), and shaded circles denote interlayer lithiums.

X-ray patterns show the basic metal oxide layer structure of Li_2MoO_3 is retained on ion exchange and that $Li_4Mo_3O_8$ has a very similar structure to Li_2MoO_3.[12]

In this work we use EXAFS to probe the local structure of the Mo^{IV}-containing molybdates, Li_2MoO_3, $Li_4Mo_3O_8$, and H_2MoO_3, and to investigate the Mo^{III}-containing $LiMoO_2$. The results show that the structures of even apparently simple compounds containing molybdenum−molybdenum bonds may still contain surprises.

Experimental Section

Syntheses. (a) Lithium Molybdates. Li_2MoO_4 was prepared from Li_2CO_3 (Fisons, 99.95%) and MoO_3 (Aldrich, 99.5%), ground together and heated at 550 °C for 24 h in an alumina crucible. Li_2MoO_3 was prepared by reduction, under flowing hydrogen at 600 °C, of Li_2MoO_4 for 48 h. $Li_4Mo_3O_8$ and $LiMoO_2$ were prepared by heating Li_2MoO_4 and Mo powder (Aldrich, 99.95%), mixed in the required stoichiometric ratios and pressed into pellets in alumina crucibles contained in sealed evacuated silica tubes. The mixtures were heated for 24 h at 500 °C and then held at 900 °C for 4 days.

(b) $Zn_2Mo_3O_8$. $Zn_2Mo_3O_8$ was prepared from ZnO (BDH AnalaR, 99.5%), MoO_3, and Mo, mixed in the required stoichiometric ratios and heated in a sealed evacuated silica tube for 24 h at 500 °C and 24 h at 900 °C. The mixture was then reground and reheated for 48 h at 900 °C.

(c) H_2MoO_3. H_2MoO_3 was prepared by refluxing, under nitrogen, 1.08 g of Li_2MoO_3 with excess (50 cm^3) 2 M H_2SO_4 for 5 h.

Sample Characterization. Powder X-ray diffraction patterns of the products were recorded using a Spectrolab Series 3000 CPS-120 X-ray diffractometer equipped with an INEL multichannel detector. The diffraction patterns of the samples matched those given in the literature.[1,9,12,14] The oxidation state of molybdenum in Li_2MoO_3 and H_2MoO_3 was determined by the reducing power analysis of Choain and Marion[15] and confirmed that these compounds contain Mo^{IV}. The quantity of lithium exchanged into the acid after the ion exchange reaction to form H_2MoO_3 was determined by atomic absorption analysis to be 99 ± 2%.

EXAFS Experiment. Mo K-edge EXAFS data were collected in transmission mode on station 9.2 at the Daresbury Laboratory SRS, using a Si[220] crystal monochromator. Ionization chambers filled with a mixture of Ar/He and Kr/He at appropriate partial pressures to optimize detector sensitivities were placed in the beam path before and behind the sample. Finely ground samples were diluted in boron nitride to give a satisfactory edge jump and absorption. Data were collected at both room temperature and 80 K. The upper limit in k was limited by an instrumental problem, which created a discontinuity in the absorption spectrum at $k = 19$ Å^{-1}.

Data Analysis

The basic equation for the interpretation of EXAFS data is

$$\chi(k) = \sum_j \frac{N_j}{kR_j^2} |f_j(\pi)| e^{-2R_j/\lambda} e^{-2\sigma_j^2 k^2} \sin(2kR_j + 2\delta + \psi_j)$$

where $\chi(k)$ is the magnitude of the X-ray absorption fine structure as a function of the photoelectron wave vector k, N_j is the coordination number, and R_j is the interatomic distance for the jth shell. δ and ψ_j are phase shifts experienced by the photoelectron, $f_j(\pi)$ is the amplitude of the photoelectron backscattering, and λ is the electron mean free path; these are calculated within EXCURV92.[16] The Debye−Waller factor is represented by $A = 2\sigma^2$ in EXCURV92.

We used the programs EXCALIB, EXBACK, and EXCURV92[16] to extract the EXAFS signal and analyze the data. Least-squares refinements of the structural parameters of our compounds were carried out against the k^3-weighted EXAFS signal to minimize the fit index

$$FI = \sum_i (k^3(\chi_i^T - \chi_i^E))^2$$

where χ_i^T and χ_i^E are the theoretical and experimental EXAFS, respectively. The results of refinements are reported in terms of the discrepancy index

$$R = (\int |(\chi^T(k) - \chi^E(k))| k^3 \, dk / \int |\chi^E(k)| k^3 \, dk) \times 100\%$$

A model compound, $Zn_2Mo_3O_8$, was used to check that the amplitudes and phase factors calculated within EXCURV92 were appropriate. Details of the number of shells and other structural parameters used in each case are given below.

Results and Discussion

The EXAFS data revealed no evidence of structural rearrangements occurring on cooling the samples to 80 K. We therefore present the results from analysis of the low-temperature data in which the effects of thermal motion have been reduced.

$Zn_2Mo_3O_8$. Information on distances out to approximately 9 Å is contained in the Fourier transform of the Mo K-edge EXAFS data collected on $Zn_2Mo_3O_8$. Interatomic distances from the single-crystal X-ray structure of Ansell and Katz[17] were used to construct a model with 14 shells. Figure 3 shows the EXAFS data, theoretical fit, and Fourier transform. The number of atoms in each shell was fixed, and R and A were refined to give the values shown in Table 1. The values of R from the single-crystal X-ray study are given for comparison, with average R's when more than one interatomic distance has been included in the shell used in EXAFS analysis. Oxygen shells are included up to 4.5 Å, and zinc and molybdenum shells are

(15) Choain, C.; Marion, F. *Bull. Soc. Chim. Fr.* **1963**, *9−10*, 212.

(16) Binsted, N.; Campbell, J. W.; Gurman, S. J.; Stephenson, P. C. *EXAFS analysis program*; Daresbury Laboratory: Daresbury, U.K., 1991.

(17) Ansell, G. B.; Katz, L. *Acta Crystallogr.* **1966**, *21*, 482.

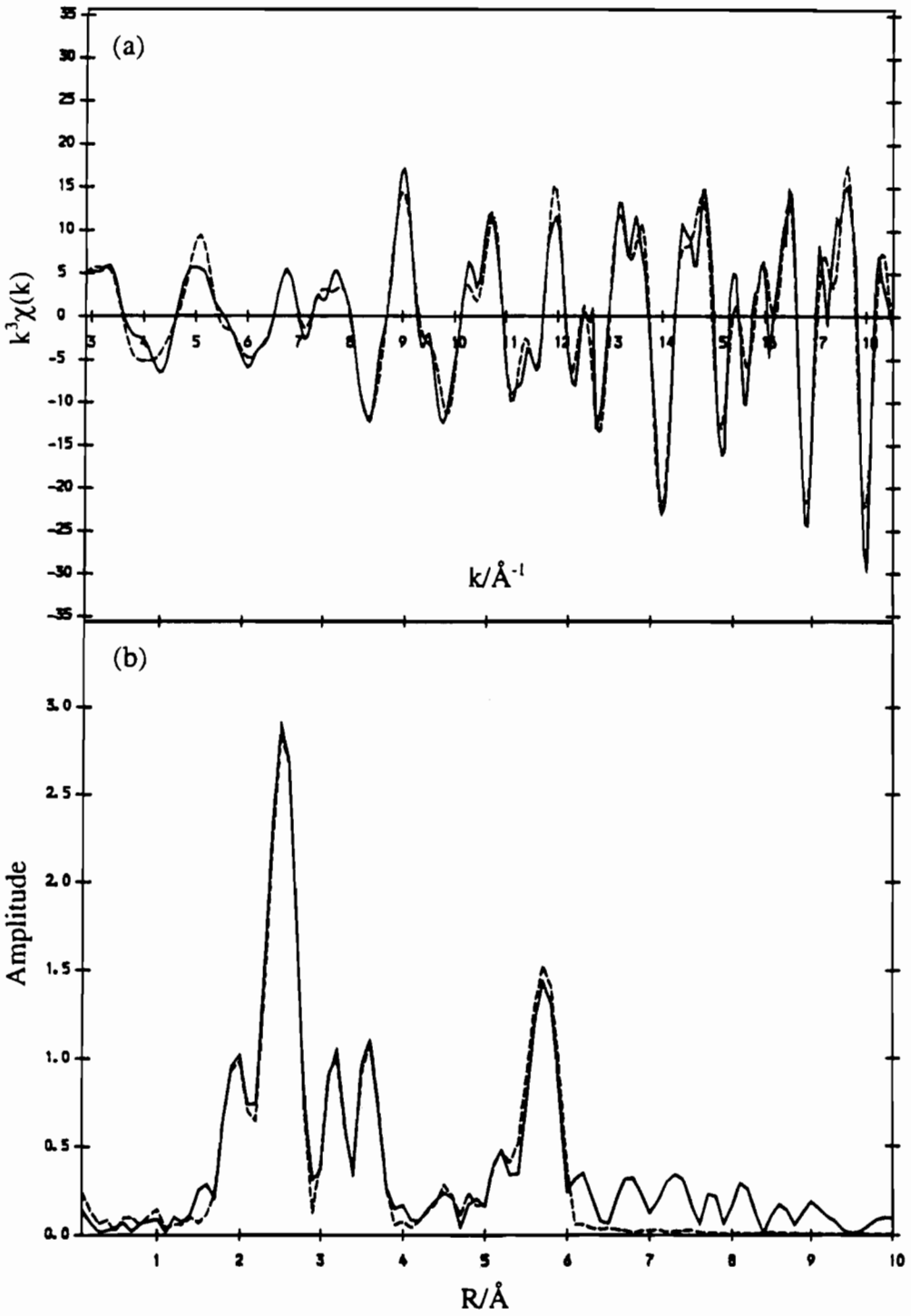

Figure 3. Mo K-edge EXAFS data for $Zn_2Mo_3O_8$: (a) k^3-weighted EXAFS (—) experimental and (- -) theoretical, R = 26.7%; (b) the Fourier transform.

included up to 6 Å (omitted shells had no statistical significance or visual effect on the calculated EXAFS signal or its Fourier transform).

There is very good agreement between the distances obtained from EXAFS data analysis and the single-crystal study, suggesting that the parameters calculated within EXCURV92 are appropriate for this work. A notable feature was the fact that it was possible to refine R and A for the six oxygens of the MoO_6 group in the four shells found in the single-crystal study. This gave the oxygen atoms a more physically-realistic temperature factor than a model constraining them to one shell. The Mo−O bond lengths can be used to calculate the molybdenum valency using the relationship $s_{Mo-O} = (d_{Mo-O}/1.882)^{-6}$, where s_{Mo-O} is the bond strength, d_{Mo-O} is the Mo−O bond length, in angstroms, and 1.882 is the empirical single-bond length derived by Brown and Wu.[18] The molybdenum valency, V, is obtained by summing the Mo−O bond strengths ($V_{Mo} = \Sigma s_{Mo-O}$). The value obtained, 4.07, is identical to that obtained using single-crystal data.

Li_2MoO_3. The Fourier transform of the Mo K-edge EXAFS data collected on Li_2MoO_3, Figure 4, shows a close similarity to that from $Zn_2Mo_3O_8$, Figure 3. Our structural model for refinement was derived from that for $Zn_2Mo_3O_8$ which, in

(18) Brown, I. D.; Wu, K. K. *Acta Crystallogr., Sect. B: Struct. Crystallogr. Cryst. Chem.* **1976**, *B32*, 1957.

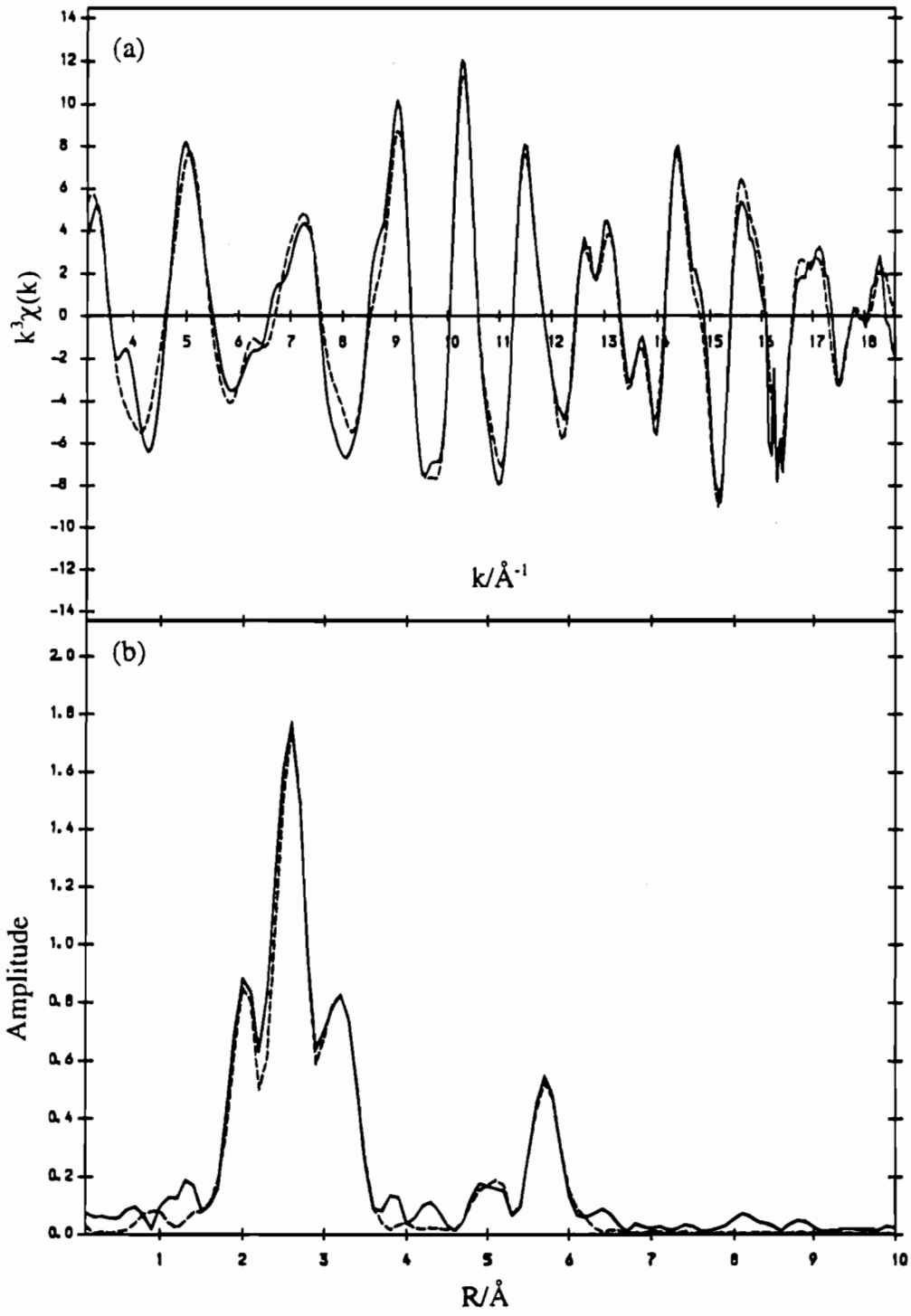

Figure 4. Mo K-edge EXAFS data for Li_2MoO_3: (a) k^3-weighted EXAFS (—) experimental and (- -) theoretical, R = 21.5%; (b) the Fourier transform.

contrast to the structure reported for Li_2MoO_3, does contain Mo_3 triangles. Refinement of the coordination number for the first molybdenum shell gave 2.2 ± 0.1. We subsequently fixed this value at 2, and this gave reasonable A factors close to those found in $Zn_2Mo_3O_8$. Attempts to model the data using other models, for example, molybdenum dimers, gave very poor agreement between the calculated and observed EXAFS signals. Numbers of Mo atoms in the shells are calculated from the statistical occupancy of $^2/_3$ for Mo sites at large distances beyond the Mo_3 triangle. The number of molybdenums in the second Mo shell is calculated by assuming a random removal of Mo_3 triangles from the ordered $Zn_2Mo_3O_8$ structure. The oxygens in the MoO_6 groups are refined as four shells as for $Zn_2Mo_3O_8$. We found that the backscattering from lithium was insignificant, and neglecting it also has the advantage of reducing the number of shells in our model. The results of the refinement are shown in Figure 4 and Table 2.

The presence of two Mo neighbors at 2.58 Å compared to 2.52 Å in $Zn_2Mo_3O_8$ is strong evidence for the presence of Mo_3 triangles in Li_2MoO_3. Alternative models, such as infinite chains, are not consistent with the other distances and must be rejected. Such chains would produce close Mo−Mo distances which have not been observed (cf. $LiMoO_2$ below). This EXAFS study therefore gives, for the first time, structural evidence for the presence of Mo_3 triangles in this material. This information cannot be obtained from Bragg diffraction experi-

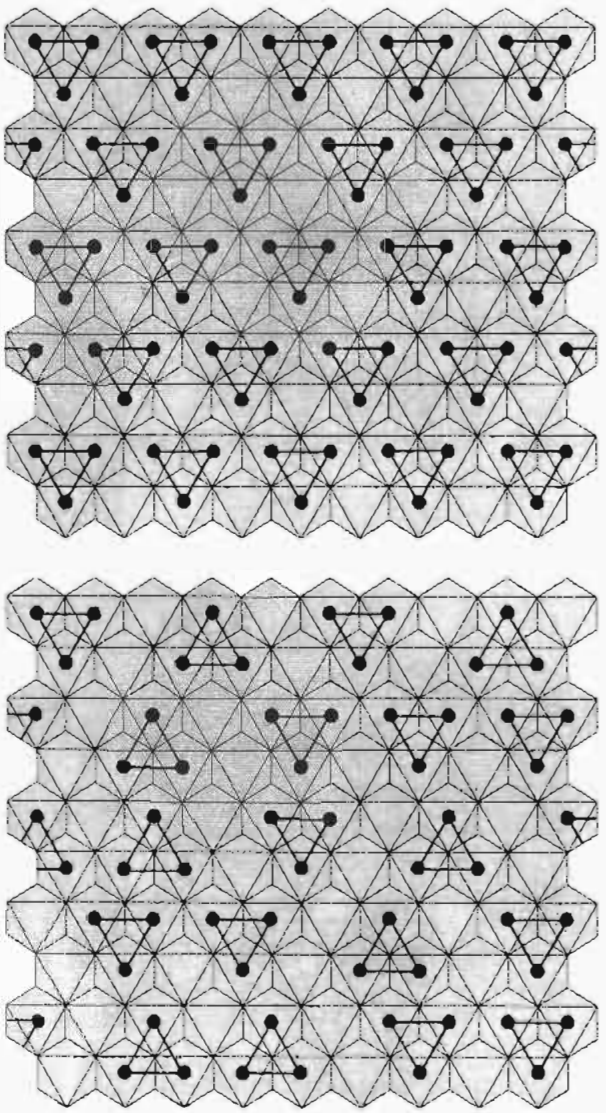

Figure 5. (a) Top: Ordered Mo_3 triangles in the $[Mo_{0.75}O_2]$ layers in $Zn_2Mo_3O_8$ (solid circles: Mo). (b) Bottom: Disordered Mo_3 triangles in the $[Mo_{2/3}O_2]$ layers in Li_2MoO_3 (solid circles: Mo).

Table 1. Occupation Numbers (N) and Distances (R) Derived from the Single-Crystal Structure of $Zn_2Mo_3O_8$ and EXAFS-Derived Distances and Debye–Waller Factors (A) for These Shells

shell	N	crystallographic-derived R/Å	EXAFS-derived R/Å	A/Å^2
Mo–O(4)	2	1.928	1.937(7)	0.0020(15)
Mo–O(1)	1	2.002	2.001(10)	0.0013(13)
Mo–O(3)	2	2.058	2.041(9)	0.0010(20)
Mo–O(2)	1	2.128	2.139(15)	0.0013(33)
Mo–Mo	2	2.524	2.525(1)	0.0020(1)
Mo··Mo	2	3.235	3.234(3)	0.0039(4)
Mo··Zn	3	3.501[a]	3.506(2)	0.0019(3)
Mo··Zn	2	3.719[a]	3.690(9)	0.0078(16)
Mo··O	8	4.658[a]	4.487(17)	0.0061(28)
Mo··Zn	2	4.982[a]	4.880(18)	0.0068(31)
Mo··Zn	3	5.189[a]	5.076(5)	0.0005(6)
Mo··Mo	8	5.081[a]	5.120(6)	0.0086(9)
Mo··Mo	8	5.756[a]	5.700(2)	0.0005(2)
Mo··Zn	3	5.523[a]	5.719(7)	0.0011(9)

[a] Average crystallographic distance.

ments because the triangles are disordered within the $[Mo_{2/3}Li_{1/3}]O_2$ layers. The disorder is a result of the impossibility of forming an ordered arrangement of triangles on the hexagonal lattice when two-thirds of the sites are occupied by molybdenum (see James and Goodenough[13]). In Figure 5a the ordered arrangement of Mo_3 triangles in $Zn_2Mo_3O_8$ is shown, and in Figure 5b we show Mo_3 units disordered in the MO_2 layer. Calculation of the molybdenum valency using bond strength vs bond length calculations gives 4.14, which is much more reasonable than the value (3.71) calculated from the atomic parameters of James and Goodenough with Mo atoms at the center of the MoO_6 octahedron.

Table 2. Occupation Numbers (N), Distances (R), and Debye–Waller Factors (A) Obtained from the EXAFS Study of Li_2MoO_3

shell	N	R/Å	A/Å^2
Mo–O(4)	2	1.936(8)	0.0114(6)
Mo–O(1)	1	1.992(10)	0.0027(15)
Mo–O(3)	2	2.052(11)	0.0055(17)
Mo–O(2)	1	2.079(26)	0.0051(41)
Mo–Mo	2	2.580(1)	0.0052(1)
Mo··Mo	1.8	3.180(2)	0.0055(2)
Mo··Mo	4	5.027(8)	0.0129(13)
Mo··Mo	4	5.225(13)	0.0162(23)
Mo··Mo	4	5.664(3)	0.0044(4)
Mo··Mo	4	5.923(29)	0.0196(54)

Table 3. Occupation Numbers (N), Distances (R), and Debye–Waller Factors (A) Obtained from the EXAFS Study of $Li_4Mo_3O_8$

shell	N	R/Å	A/Å^2
Mo–O(4)	2	1.954(9)	0.0086(18)
Mo–O(1)	1	1.994(11)	0.0016(13)
Mo–O(3)	2	2.034(7)	0.0051(12)
Mo–O(2)	1	2.116(13)	0.0037(21)
Mo–Mo	2	2.560(1)	0.0041(1)
Mo··Mo	2	3.170(2)	0.0049(3)
Mo··Mo	8	4.976(10)	0.0180(17)
Mo··Mo	8	5.650(3)	0.0041(2)

Table 4. Occupation Numbers (N), Distances (R), and Debye–Waller Factors (A) Obtained from the EXAFS Study of H_2MoO_3

shell	N	R/Å	A/Å^2
Mo–O(4)	2	1.909(3)	0.0018(6)
Mo–O(1)	1	2.015(8)	0.0016(14)
Mo–O(3)	2	2.041(9)	0.0064(21)
Mo–O(2)	1	2.171(7)	0.0015(14)
Mo–Mo	2	2.506(1)	0.0040(1)
Mo··Mo	1.8	3.313(8)	0.0154(15)

Table 5. Occupation Numbers (N), Distances (R), and Debye–Waller Factors (A) Obtained from the EXAFS Study of $LiMoO_2$

shell	N	R/Å	A/Å^2
Mo–O	6	2.024(4)	0.0111(7)
Mo–Mo	2	2.561(2)	0.0049(2)
Mo–Mo	2	2.709(2)	0.0067(3)
Mo··Mo	2	3.162(2)	0.0037(2)
Mo··Mo	2	4.435(10)	0.0102(16)
Mo··Mo	4	5.001(7)	0.0112(14)
Mo··Mo	6	5.211(4)	0.0066(5)
Mo··Mo	2	5.350(4)	0.0006(4)
Mo··Mo	4	5.647(3)	0.0014(3)
Mo··Mo	6	5.827(28)	0.0208(51)

$Li_4Mo_3O_8$. The striking resemblance of both the EXAFS signal and Fourier transform of $Li_4Mo_3O_8$ to those of Li_2MoO_3 (Figure 6) suggests that the structures are closely related. This can be seen more clearly when the formulas are expressed relative to one MO_2 layer, when Li_2MoO_3 becomes $Li[Mo_{2/3}Li_{1/3}]O_2$, and $Li_4Mo_3O_8$ can be written as $Li[Mo_{3/4}V_{1/4}]O_2$ or $Li_{3/4}[Mo_{3/4}Li_{1/4}]O_2$, where V is a vacant metal site. The $Li_4Mo_3O_8$ model was modified to take account of the increased Mo occupation number in the layer and refined. As in the case

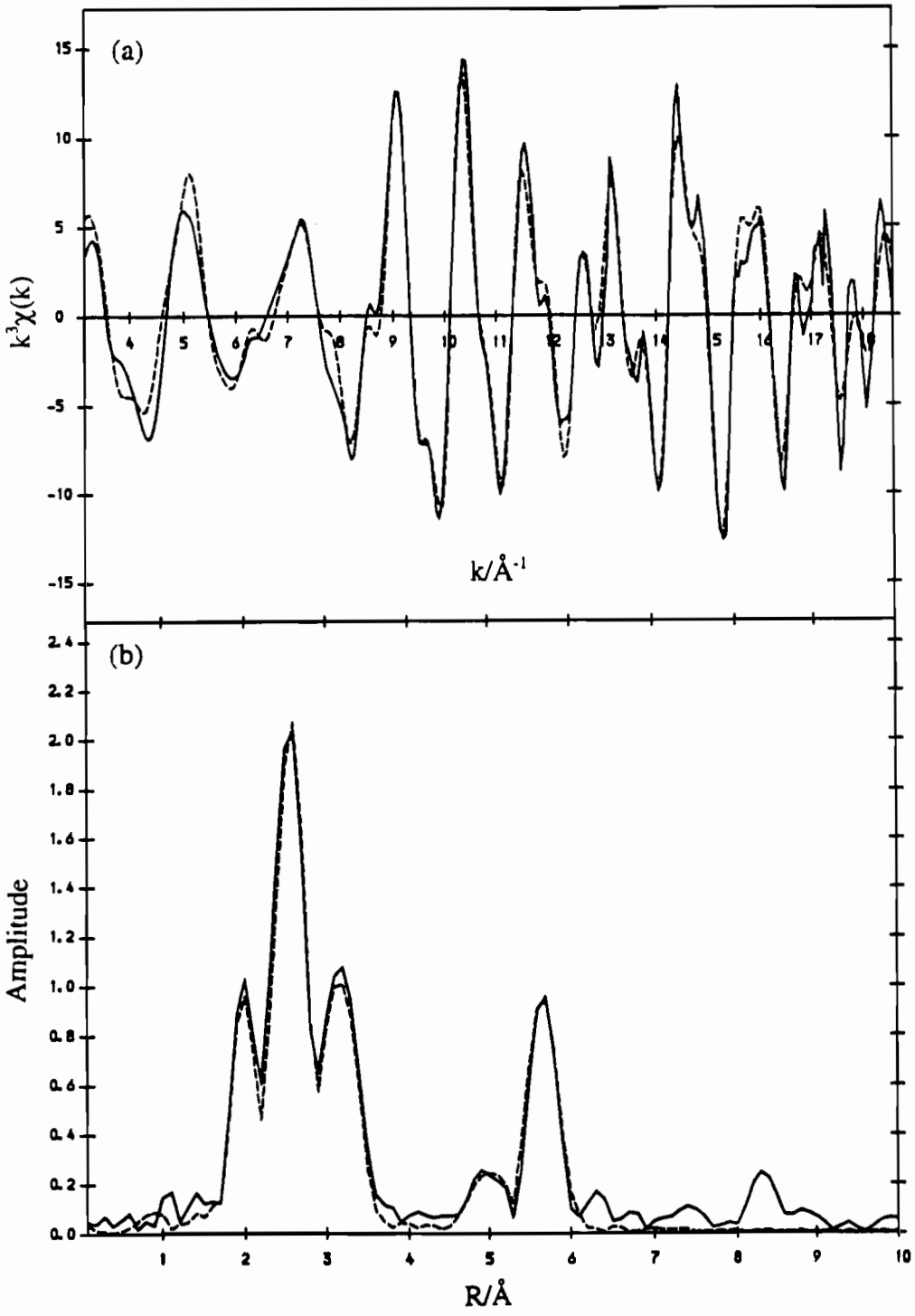

Figure 6. Mo K-edge EXAFS data for $Li_4Mo_3O_8$: (a) k^3-weighted EXAFS (—) experimental and (- -) theoretical, R = 25.8%; (b) the Fourier transform.

of Li_2MoO_3, refinement of N for the first shell of molybdenum gave values very close to 2 (2.1 ± 0.1), and this was fixed at 2 for the final refinements. The results are presented in Table 3. $Li_4Mo_3O_8$ clearly contains Mo_3 triangles, and bond valence calculations give a Mo valency of 4.05, in good agreement with the expected value of 4. The occupation number of $^3/_4$ for Mo in the hexagonal sheets should permit an ordered arrangement of triangles (as in $Zn_2Mo_3O_8$), but no evidence for this is seen in powder X-ray diffraction measurements.[12] In this compound it may be that ordering within the layers occurs but interlayer interactions are too weak to cause long-range ordering.

H_2MoO_3. The Fourier transform of the EXAFS data for H_2MoO_3, Figure 7, shows the loss of long-range order which has occurred during the ion exchange reaction. This is also evidenced by the loss of crystallinity which is seen in powder X-ray studies.[12,14] However, the short-range order can still be modeled using Mo_3 triangles, and the Mo−O distances in the MoO_6 octahedron remain similar to those observed in $Zn_2Mo_3O_8$, Li_2MoO_3, and $Li_4Mo_3O_8$. Refinement of N for the first two molybdenum shells gave 1.9 ± 0.1 and 1.9 ± 0.2, respectively, in excellent agreement with the values of 2 and 1.78 expected for disordered triangles. These values were fixed at the theoretical values for the final refinements. Other models gave much inferior fits. Table 4 gives the refined parameters. The molybdenum valence calculated from the refined Mo−O bond distances is 4.15.

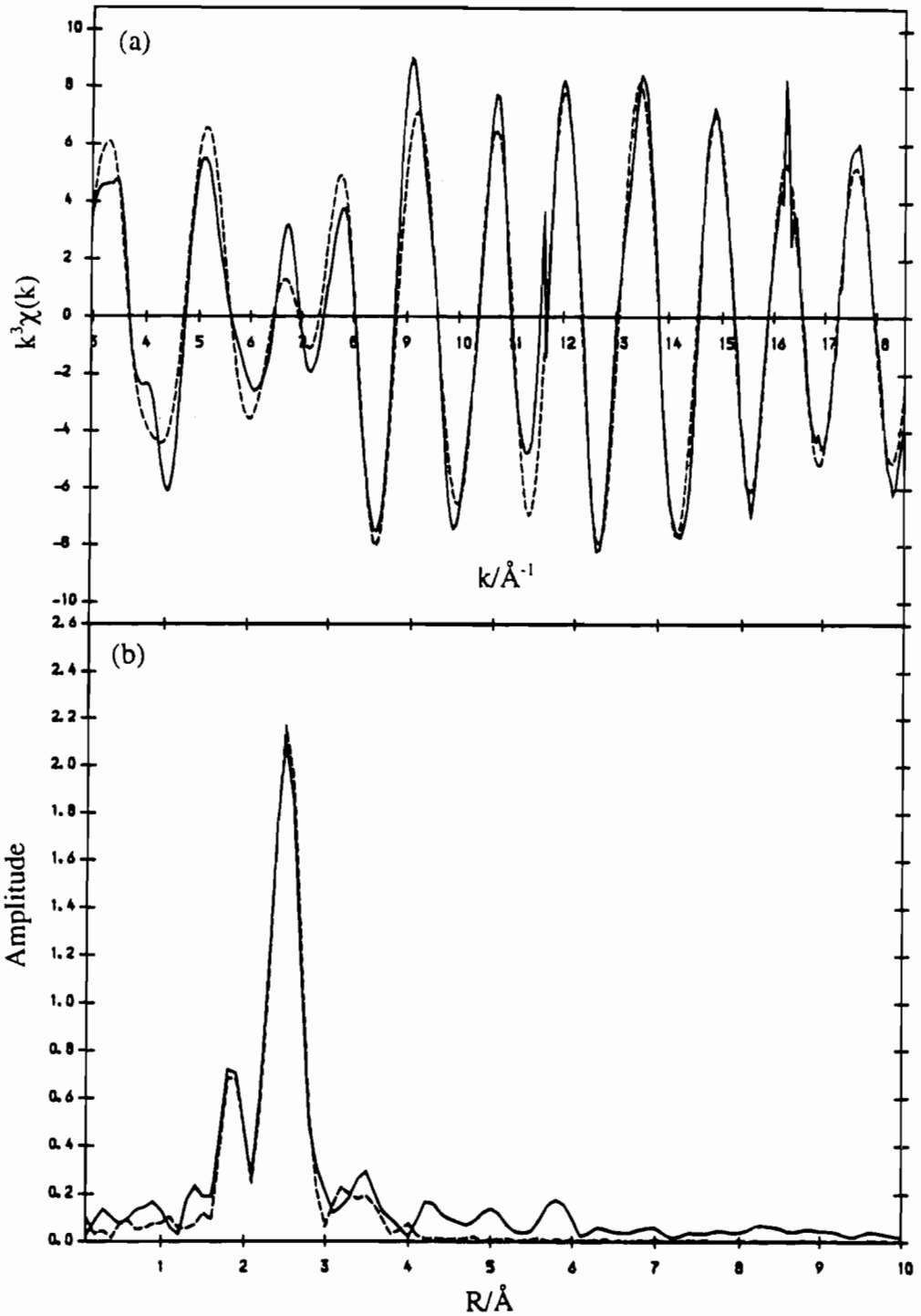

Figure 7. Mo K-edge EXAFS data for H_2MoO_3: (a) k^3-weighted EXAFS (—) experimental and (- -) theoretical, R = 22.4%; (b) the Fourier transform.

$LiMoO_2$. Initial attempts to fit the EXAFS data using the structural parameters presented by Aleandri and McCarley[9] showed that their model, which yields six equal Mo−Mo bond lengths, was far from the truth. Inspection of the Fourier transform showed a short Mo−Mo distance, similar to that in $Zn_2Mo_3O_8$, and an intermediate Mo−Mo bond distance of 2.7 Å not seen in any of the materials above. A good fit to the data was obtained by using a model with two short (2.56 Å), two medium (2.71 Å), and two long (3.16 Å) Mo−Mo bonds to the six nearest molybdenums in the MoO_2 sheet. These distances and coordination numbers are consistent with the formation of Mo−Mo-bonded zigzag chains. Refinement of N's for the first three molybdenum shells gave 2.3 ± 0.3, 1.5 ± 0.2, and 2.3 ± 0.2, respectively, in reasonable agreement with the model. Other chain models[19] based on the metal clustering found in $ReSe_2$[20] (a d^3 system like Mo^{III}) and ternary sulfides gave almost as satisfactory fits to the EXAFS signal, but with less believable A factors for molybdenum. It is difficult to discriminate between alternative chain models using EXAFS, because of the degree of uncertainty in coordination number, and the situation is further complicated by the necessity of explaining why this system is disordered. We therefore used the basic molybdenum chain, which has analogues elsewhere

(19) We thank the reviewer who drew our attention to this other possibility.
(20) Alcock, N. W.; Kjekshus, A. *Acta Chem. Scand.* **1965**, *19*, 79.

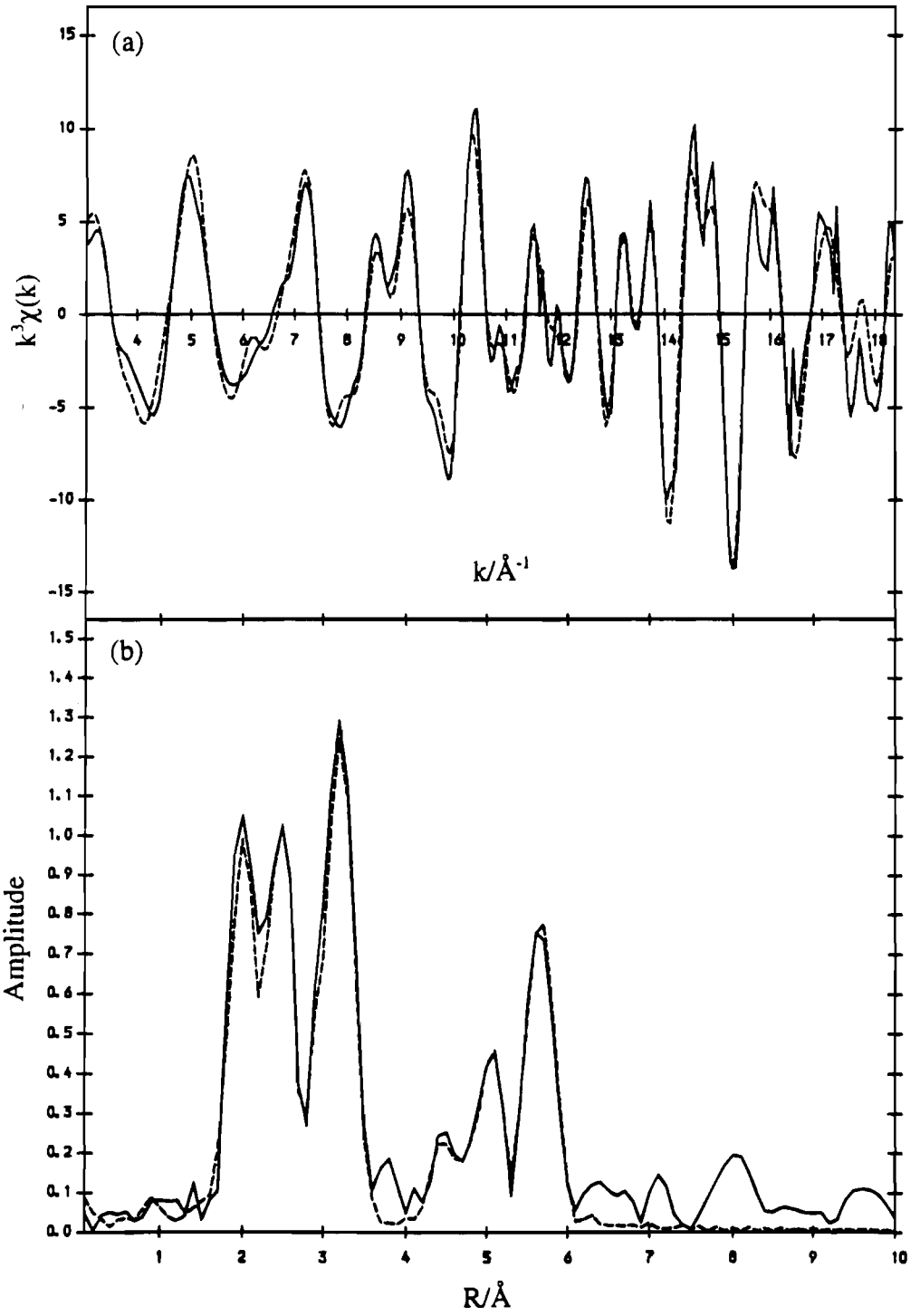

Figure 8. Mo K-edge EXAFS data for $LiMoO_2$: (a) k^3-weighted EXAFS (—) experimental and (- -) theoretical, R = 27.3%; (b) the Fourier transform.

in molybdenum oxide chemistry, as a basis for our model. The Mo−O bond distances in the MoO_6 unit were modeled using a single shell and the remainder of the model derived from that for Li_2MoO_3. The results of fitting the EXAFS signal to a model with 10 shells, with the parameters given in Table 5, are given in Figure 8.

The Mo−Mo distances are similar to those found for the Mo−Mo-bonded zigzag chains in $Li_{0.74}MoO_2$ and $NaMo_2O_4$. The short Mo−Mo distances in the three compounds are 2.561, 2.549, and 2.535 Å for $LiMoO_2$, $Li_{0.74}MoO_2$, and $NaMo_2O_4$, respectively. The major difference occurs in the next shortest Mo−Mo distances, which are 2.709, 2.881, and 2.893 Å for $LiMoO_2$, $Li_{0.74}MoO_2$, and $NaMo_2O_4$, respectively. The much shorter bond length for $LiMoO_2$ arises because molybdenum is in a lower oxidation state and more electrons are available for Mo−Mo bonding. The lack of long-range order (no evidence in the powder X-ray pattern or neutron study of Aleandri and McCarley) arises because the repeat distance along the chain is incommensurate with the O−O repeat. The shorter Mo−Mo bond length of 2.709 Å cannot be accommodated in a periodic structure with close-packed oxide layers. The chains must break or twist to relax the strain and thus form the disordered Mo layers. Figure 9 shows a possible disordered arrangement of short chains in the MoO_2 layers. In this picture, the molybdenum−molybdenum coordination numbers would no longer be expected to have the ideal values of the inifinite-chain model.

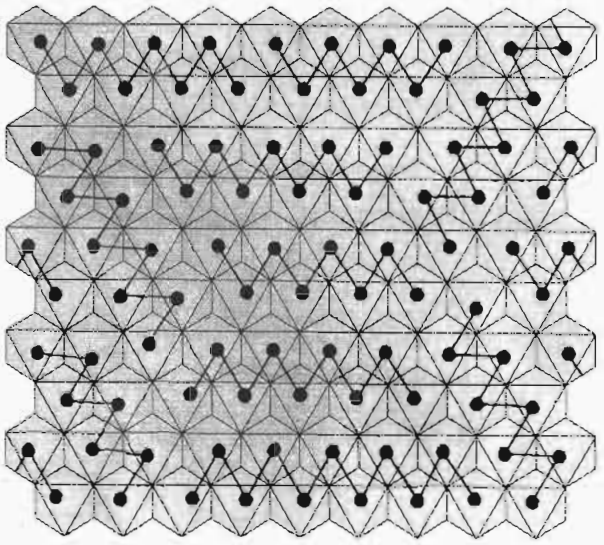

Figure 9. Disordered Mo, chains in the $[MoO_2]$ layers in $LiMoO_2$ (solid circles: Mo).

The refined N values above go some way to supporting the broken-chain model, since the coordination number along the chain direction refines to less than 2 (1.5), as expected, and the number of molybdenums at ~3.2 Å increases from 2 to 2.3. However, we believe that pursuing this line could lead to overinterpretation of the EXAFS data and believe other experiments are necessary to discriminate definitively between the various possible chain models. Calculation of the molybdenum valency from the metal−oxygen bond lengths gives a value of 3.88; this does not agree with the value of 3 expected. The poor agreement may arise from the fact that only a single oxygen shell can be refined.

Conclusions

Analysis of EXAFS data has allowed us to obtain information on Mo−Mo bonding in a number of apparently simple compounds where Bragg diffraction has failed. Metal−metal bonding has important structural consequences, and nature has found ingenious ways of accommodating the bonding requirements within otherwise periodic lattices.

Acknowledgment. We thank the EPSRC for the provision of EXAFS facilities and a studentship for I.D.F.

IC940923T